On the Delay and Gaussian Random Scattering Estimation for GNSS-R Applications

Filippo Torrisi
ISAE-SUPAERO
Toulouse, France
filippo.torrisi@isae.fr

Corentin Lubeigt
Météo-France
Toulouse, France
corentin.lubeigt@meteo.fr

Jordi Vilà-Valls
ISAE-SUPAERO
Toulouse, France
jordi.vila-valls@isae.fr

Eric Chaumette
ISAE-SUPAERO
Toulouse, France
eric.chaumette@isae.fr

***Abstract*—The delay-Doppler map is the primary observable used in most Global Navigation Satellite System (GNSS) reflectometry retrieval algorithms. The standard underlying assumption is to consider a conditional (deterministic) signal model, whereby all unknown parameters are assumed to be deterministic. However, a Gaussian random surface scattering model, leading to an unconditional (stochastic) signal model (USM), may be more informative. To assess the potential benefits of the USM, we first consider delay and Gaussian source mean and variance estimation. For these, we derive compact, closed-form, unconditional Cramér–Rao bound (CRB) expressions and the corresponding maximum likelihood estimators. The results are validated with a representative GNSS signal.**

***Index Terms*—Unconditional CRB, unconditional MLE, delay estimation, Gaussian scattering, band-limited signals.**

I. Introduction

Global Navigation Satellite Systems (GNSS) reflectometry (GNSS-R) is a powerful way to retrieve information from a reflecting surface (for Earth observation) by exploiting GNSS as signals of opportunity [1–3]. There exist a plethora of applications and retrieval methods depending on the sensing platform, the satellite geometry, and the reflecting surface, which may lead to either altimetric information or the reflecting surface characterization (e.g., roughness, surface wind, soil moisture, sea-ice salinity or snow water content) [4, 5].

In dual-antenna configurations the main input to the different retrieval methods is the delay-Doppler map (DDM) of the scattered signal (i.e., an image of the scattering coefficient in the delay-Doppler domain), which is obtained by cross-correlation of a local GNSS code replica and the signal from the down-looking antenna at different delays and Doppler frequency shifts. The DDM observable strongly depends on the nature of the reflecting surface, which may induce a diffuse scattering, a coherent reflection, or a mixed diffuse/coherent reflection [1, 4, 5]. This led to several studies focusing on the analysis, detection and characterization of the reflected signal coherence [6–16]. In particular, it was shown in [7] that by computing the variance of DDM observables it was possible to decouple the diffuse and coherent scattering contributions, allowing to process the latter without the distortion induced by the former, leading to possible new applications (e.g., improved resolution for altimetry, or wave periods estimation).

From a signal processing perspective, the underlying assumption to build a DDM (scattering coefficients such as the complex amplitude of the different cross-correlation points), and to estimate the delay and Doppler of the specular point for coherent reflections [17], is to consider a Gaussian conditional signal model (CSM) [18]. That is, for the reflected signal: delay, Doppler, complex amplitude, and noise power are assumed to be unknown deterministic parameters. In this case: i) the conditional Cramér-Rao bound (CRB_c) [19, 20] provides the optimal performance in the mean square error (MSE) sense, and ii) the conditional maximum likelihood (ML) estimator (CMLE) is known to be asymptotically efficient (i.e., in the large sample and/or high signal-to-noise (SNR) regimes [18, 21]). The question that ignited this work, in line with the DDM variance estimator introduced in [6, 7] is: considering a Gaussian prior for the scattering, does one obtain additional useful information for GNSS-R applications?

In contrast to the standard (deterministic) CSM case, an unconditional (stochastic) signal model (USM) [18] needs to be considered to properly account for a random surface scattering. In this study, a simplified USM, assuming a known and compensated Doppler shift, is introduced to demonstrate the interest of that approach. With those assumptions, the goals of this contribution are i) to derive closed-form unconditional CRB (CRB_u) expressions for the estimation of the Gaussian scattering mean and variance and signal delay, and ii) to assess the performance of the corresponding unconditional ML estimator (UMLE) [22]. The results are validated with a representative band-limited GNSS signal.

II. Signal model and problem formulation

The transmission of a GNSS band-limited signal $s(t)$ with bandwidth B, from a GNSS satellite T to a GNSS-R receiver R with two antennas is considered. The signal of interest is the signal that goes through a surface reflection and is collected by the down-looking antenna. If the T-to-R distance is constant during the observation time (constant propagation delay τ), the baseband output of the receiver front-end is $y(t) = \alpha s(t-\tau) + n(t)$, where $n(t)$ is a complex white

Funded by the European Union (EU) under the GLITTER HORIZON–MSCA–2022–DN grant. Views and opinions expressed are however those of the authors only and do not necessarily reflect those of the EU, and the EU cannot be held responsible for them. This work was also partially supported by the AID projects 2023.65.0083 and 2025.65.0026.

Gaussian noise with variance σ_n^2, and α is a complex amplitude that mainly depends on i) the reflecting surface, and ii) the transmitted signal power, T and R antenna gains and polarizations, and the propagation path length between T and R [1, 23, 24]. The discrete signal model is built from K snapshots, each one with N samples at $T_s = 1/F_s$, and $F_s \geq B$ the Hilbert filter bandwidth,

$$\mathbf{y}_k = \alpha_k \mathbf{s}(\tau) + \mathbf{n}_k,\ \mathbf{n}_k \sim \mathcal{CN}(\mathbf{0}, \sigma_n^2 \mathbf{I}_N),\ k = 1, \ldots, K, \quad (1)$$

with $\mathbf{y}_k^T = (y_k(T_s), \ldots, y_k(NT_s))$ the received signal samples, $\mathbf{s}^T(\tau) = (s(T_s - \tau), \ldots, s(NT_s - \tau))$ the delayed transmitted signal samples, $\mathbf{n}_k^T = (n_k(T_s), \ldots, n_k(NT_s))$. Depending on the definition of α_k, the following signal models can be considered:

- Standard noncoherent case: α_k is a complex parameter that changes between snapshots. The CSM is then,

$$\mathbf{y}_k \sim \mathcal{CN}(\alpha_k \mathbf{s}(\tau), \sigma_n^2 \mathbf{I}_N),\ k = 1, \ldots, K, \quad (2)$$

  where the unknown deterministic parameters to be estimated are σ_n^2, $\boldsymbol{\alpha}^T = (\alpha_1, \ldots, \alpha_K)$ and τ.
- USM: the case of interest, where a complex Gaussian prior is assumed for α_k. Then, for $k = 1, \ldots, K$,

$$\alpha_k \sim \mathcal{CN}(\mu_\alpha, \sigma_\alpha^2),\ \mu_\alpha = \rho e^{j\varphi}, \quad (3a)$$

$$\mathbf{y}_k \sim \mathcal{CN}(\mathbf{m}, \mathbf{C}),\ \mathbf{m} = \mu_\alpha \mathbf{1}_N, \quad (3b)$$

$$\mathbf{C} = \sigma_\alpha^2 \mathbf{s}(\tau)\mathbf{s}^H(\tau) + \sigma_n^2 \mathbf{I}_N, \quad (3c)$$

  where $\rho \in \mathbb{R}^+$ and $0 \leq \varphi \leq 2\pi$, and the unknown parameters to be estimated are now $\boldsymbol{\theta}^T = (\sigma_n^2, \sigma_\alpha^2, \rho, \varphi, \tau)$, for which the corresponding CRB and UMLE are needed.

III. Conditional and Unconditional Maximum Likelihood Estimators

A. Background on standard (CMLE) processing

To build a DDM the standard processing is to perform the cross-correlation of a local signal replica and the signal recorded from the down-looking antenna. To build that map, the correlation is performed at different delays and Doppler frequency shifts, first in a coherent manner (the coherent integration time depends on the GNSS signal used, i.e., because of the code length and bit transitions), and then averaged or noncoherently integrated [25]. Regarding the coherent integration step, it is well known that the delay CMLE is given by the maximum of the cross-correlation. In contrast, the second step needs to consider (2). With $\|\mathbf{s}\|^2 \triangleq \mathbf{s}^H\mathbf{s}$, and the correlation function $r_k(\tau) = \mathbf{s}^H(\tau)\mathbf{y}_k$, the noncoherent CMLEs are (subscript c for conditional),

$$\widehat{\tau}_c = \arg\max_\tau \sum_{k=1}^K |r_k(\tau)|^2, \quad (4)$$

$$\widehat{\sigma}_{n,c}^2 = \frac{1}{KN} \sum_{k=1}^K \left(\|\mathbf{y}_k\|^2 - \frac{|r_k(\widehat{\tau}_c)|^2}{\|\mathbf{s}\|^2} \right), \quad (5)$$

$$\widehat{\alpha}_{k,c} = \frac{r_k(\widehat{\tau}_c)}{\|\mathbf{s}\|^2} \text{ (for each snapshot)}. \quad (6)$$

Notice that the mean and variance of the complex vector $\boldsymbol{\alpha}$ are not directly available through the CMLE, but one may compute the sample mean and sample variance from individual $\widehat{\alpha}_{k,c}$ as,

$$\widehat{\mu}_{\alpha,c} = \frac{1}{K} \sum_{k=1}^K \widehat{\alpha}_{k,c};\ \widehat{\sigma}_{\alpha,c}^2 = \frac{1}{K-1} \sum_{k=1}^K |\widehat{\alpha}_{k,c} - \widehat{\mu}_{\alpha,c}|^2. \quad (7)$$

B. Unconditional ML Estimators

In this section, the UMLE expressions that will be used to validate the CRBs derived in Section IV are presented. Given the USM in (3), the minimization of the negative log-likelihood leads to (subscript u for unconditional),

$$\widehat{\tau}_u = \arg\min_\tau \{C_u(\tau)\}, \quad (8)$$

$$C_u(\tau) = \left(\sum_{k=1}^K \left(\|\mathbf{y}_k\|^2 - \frac{|r_k(\tau)|^2}{\|\mathbf{s}\|^2} \right) \right)^{N-1} \times \left(\sum_{k=1}^K \left| r_k(\tau) - \bar{r}(\tau) \right|^2 \right), \quad (9)$$

where $\bar{r}(\tau) = \frac{1}{K} \sum_{k=1}^K r_k(\tau)$. The noise power UMLE is,

$$\widehat{\sigma}_{n,u}^2 = \frac{1}{K(N-1)} \sum_{k=1}^K \left(\|\mathbf{y}_k\|^2 - \frac{|r_k(\widehat{\tau}_u)|^2}{\|\mathbf{s}\|^2} \right), \quad (10)$$

and the Gaussian noise scattering mean and variance UMLEs,

$$\widehat{\mu}_{\alpha,u} = \frac{1}{K} \sum_{k=1}^K \frac{r_k(\widehat{\tau}_u)}{\|\mathbf{s}\|^2} = \frac{\bar{r}(\widehat{\tau}_u)}{\|\mathbf{s}\|^2}, \quad (11)$$

$$\widehat{\sigma}_{\alpha,u}^2 = \frac{1}{K(N-1)} \sum_{k=1}^K \left(N \frac{|r_k(\widehat{\tau}_u)|^2}{\|\mathbf{s}\|^4} - \frac{\|\mathbf{y}_k\|^2}{\|\mathbf{s}\|^2} \right) - \frac{|\widehat{\mu}_{\alpha,u}|^2}{\|\mathbf{s}\|^2}.$$

IV. Closed-Form Unconditional CRB

Given the USM in (3), the corresponding CRB_u for the estimation of $\boldsymbol{\theta}^T = (\sigma_n^2, \sigma_\alpha^2, \rho, \varphi, \tau)$ is now derived. For complex Gaussian observations, the Fisher information matrix (FIM) entries can be obtained from the Slepian–Bangs formula,

$$[\mathbf{F}(\boldsymbol{\theta})]_{k,\ell} = 2\Re \left\{ \left(\frac{\partial \mathbf{m}}{\partial \theta_k} \right)^H \mathbf{C}^{-1} \left(\frac{\partial \mathbf{m}}{\partial \theta_\ell} \right) \right\} + \text{Tr} \left(\mathbf{C}^{-1} \frac{\partial \mathbf{C}}{\partial \theta_k} \mathbf{C}^{-1} \frac{\partial \mathbf{C}}{\partial \theta_\ell} \right). \quad (12)$$

It can be shown that the FIM takes the following form:

$$\mathbf{F}(\boldsymbol{\theta}) = K \begin{bmatrix} w_n & w_{\alpha,n} & 0 & 0 & 0 \\ w_{\alpha,n} & w_\alpha & 0 & 0 & 0 \\ 0 & 0 & w_\rho & 0 & 0 \\ 0 & 0 & 0 & w_\varphi & w_{\tau,\varphi} \\ 0 & 0 & 0 & w_{\tau,\varphi} & w_\tau \end{bmatrix}, \quad (13)$$

$$w_\alpha = \frac{\beta^2}{(\sigma_\alpha^2)^2 (1+\beta)^2}, w_{\alpha,n} = \frac{\beta}{\sigma_\alpha^2 \sigma_n^2 (1+\beta)^2}, \quad (14)$$

$$w_n = \frac{N}{(\sigma_n^2)^2} - \frac{\beta(2+\beta)}{(\sigma_n^2)^2 (1+\beta)^2}, w_\rho = \frac{2\beta}{\sigma_\alpha^2 (1+\beta)}, \quad (15)$$

$$w_\varphi = \frac{2\gamma}{1+\beta}, w_{\tau,\varphi} = \frac{2\gamma}{(1+\beta)} \frac{w_3}{w_1}, \quad (16)$$

$$w_\tau = \frac{2}{1+\beta}\left(\gamma\frac{W_{33}}{w_1} + \beta(\gamma+\beta)\left(\frac{W_{33}}{w_1} - \frac{|w_3|^2}{w_1^2}\right)\right), \quad (17)$$

where, $\beta = \sigma_\alpha^2\|\mathbf{s}\|^2/\sigma_n^2$, $\gamma = \rho^2\|\mathbf{s}\|^2/\sigma_n^2$, and $w_1 = \|\mathbf{s}\|^2/F_s$, $w_3 = \mathbf{s}^H\mathbf{\Lambda}\mathbf{s}/F_s$, $W_{33} = F_s\mathbf{s}^H\mathbf{V}\mathbf{s}$ were introduced in [20]. The definition of $\mathbf{\Lambda}$ and $\mathbf{V}$ are recalled hereafter:

$$[\mathbf{\Lambda}]_{k,\ell} = \begin{cases} 0 & \text{if } k=\ell, \\ \frac{(-1)^{|k-\ell|}}{k-\ell} & \text{else.} \end{cases} \quad (18)$$

$$[\mathbf{V}]_{k,\ell} = \begin{cases} \pi^2/3 & \text{if } k=\ell, \\ \frac{2(-1)^{|k-\ell|}}{(k-\ell)^2} & \text{else.} \end{cases} \quad (19)$$

The FIM (13) being block diagonal, its inverse is easily obtained, yielding the following closed-form expressions:

$$\mathrm{CRB}_u(\tau) = \frac{1+\beta}{2K(\gamma+\beta(\gamma+\beta))\left(\frac{W_{33}}{w_1} - \frac{|w_3|^2}{w_1^2}\right)}, \quad (20)$$

$$\mathrm{CRB}_u(\sigma_\alpha^2) = \frac{\left(\sigma_\alpha^2\right)^2\left(1+(N-1)\left(1+\beta\right)^2\right)}{K(N-1)\beta^2}, \quad (21)$$

$$\mathrm{CRB}_u(\rho) = \frac{1+\beta}{2K\gamma}\sigma_\alpha^2, \quad (22)$$

$$\mathrm{CRB}_u(\varphi) = \frac{1+\beta}{2K\gamma} + \mathrm{CRB}_u(\tau)\frac{|w_3|^2}{w_1^2}, \quad (23)$$

$$\mathrm{CRB}_u(\sigma_n^2) = \frac{(\sigma_n^2)^2}{K(N-1)}. \quad (24)$$

V. Validation

To validate the proposed CRB, and assess the performance of the corresponding estimators, a simulated GPS L1 C/A signal sampled at 4 MHz is considered. The MSE for the estimation of $\boldsymbol{\theta}$ is obtained from 1000 Monte Carlo runs. The SNR at the output of the matched filter for a single snapshot is defined as $\mathrm{SNR}_{\text{out}} = P\|s\|^2/\sigma_n^2$, where $P = \rho^2 + \sigma_\alpha^2$ is the total averaged power.

In order to assess the impact of the different parameters of interest on the estimation performance, the following parameter is introduced as in [26]:

$$\epsilon = \frac{\rho^2}{P} \in (0,1). \quad (25)$$

The parameter ϵ can be seen as the coherent fraction of the power. When ϵ values are above 0.5 there is a smaller contribution from σ_α^2 compared to ρ, and vice versa. That formulation allows to move from the standard zero-mean USM ($\epsilon = 0, \rho = 0$) to the (coherent) CSM ($\epsilon = 1, \sigma_\alpha^2 = 0$).

All the figures related to the estimation of σ_α^2 and ρ have been normalized with respect to the power P. Consequently, they display the Normalized MSE (NMSE) and CRB (NCRB).

Figures 1 and 2 present the MSE of the UMLE of the time delay τ, the amplitude mean ρ and variance σ_α^2, with respect to the number of snapshots K, the $\mathrm{SNR}_{\text{out}}$ and ϵ. For the MSE of the time-delay, only the CRB for $\epsilon = 1$ is displayed as the CRBs for the considered values of $\mathrm{SNR}_{\text{out}}$ and number of snapshots K are very close to each other.

In these figures, when ϵ is closer to 1, the UMLE performs better for the estimation of ρ and σ_α^2, while for the estimation of τ, they are all asymptotically equivalent. That does not come as a surprise: when the total power P is fixed, a value of ϵ closer to 1 means a lower variance. In that case, the parameter σ_α^2 contributes less to the total power and the amplitude randomness decreases as well, while the parameter ρ increasing the power does not add randomness.

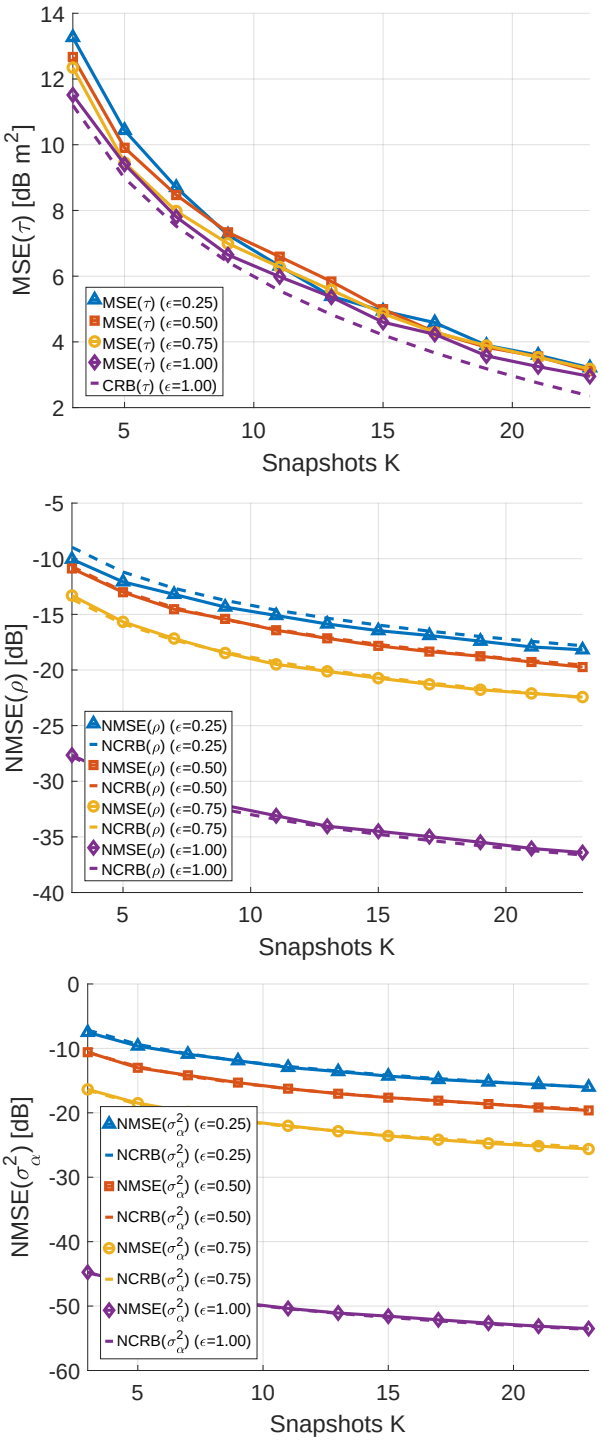

Figure 1: Comparison of the UMLE and CRB. (Top) MSE for the delay τ; (Middle) NMSE for the mean ρ; (Bottom) NMSE for the variance σ_α^2; versus the number of snapshots K (at $\mathrm{SNR}_{\text{out}} = 20$ dB), for different ϵ.

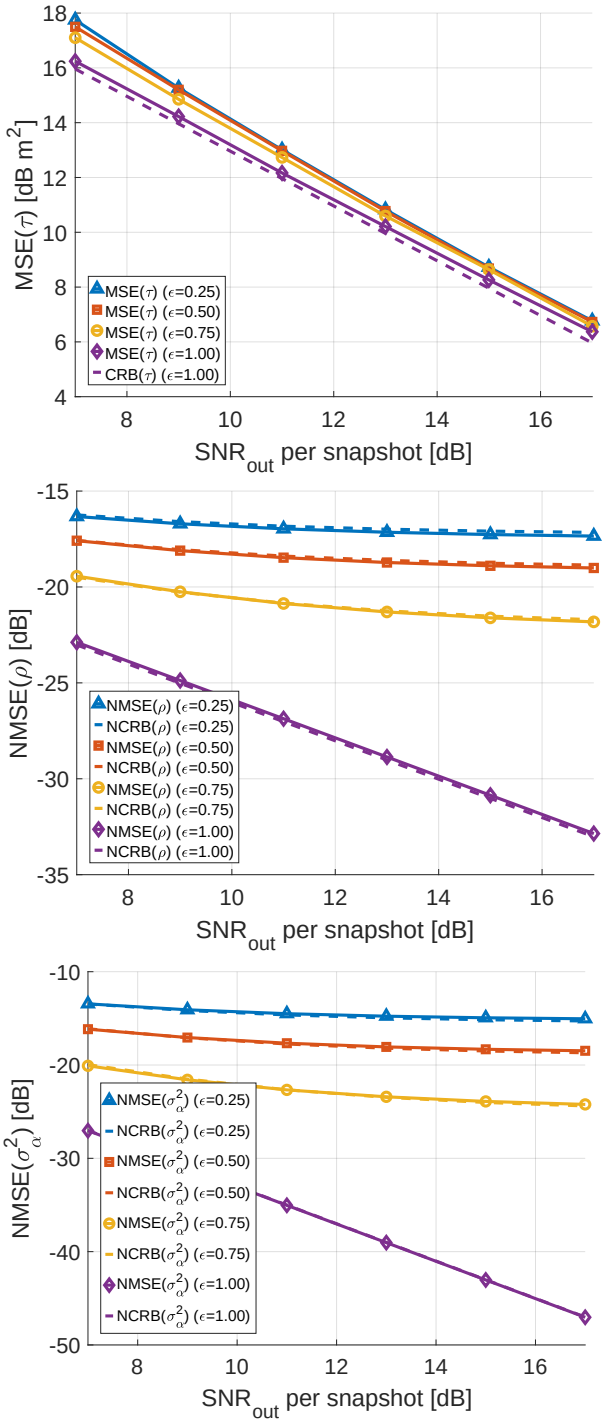

Figure 2: Comparison of the UMLE and CRB. (Top) MSE for the delay τ; (Middle) NMSE for the mean ρ; (Bottom) NMSE for the variance σ_α^2; versus SNRout (at $K = 20$), for different values of parameter ϵ.

From Figures 1 and 2, it clearly appears that the considered MSEs reach the proposed CRB. This result validates the CRB expressions derived in Section IV.

By setting $\epsilon = 1$, one ends up trying to estimate a zero-valued power variance where there is no need to estimate it. In that case, the CMLE seems more appropriate, but it may be interesting to estimate σ_α^2 even though it is null. Figure 3 presents a comparison between the CMLE (7) and the UMLE (11) for the estimation of σ_α^2 in the case where $\sigma_\alpha^2 = 0$ ($\epsilon = 1$). Interestingly, this figure shows that it might be worth implementing the UMLE rather than rely on the CMLE for the estimation of a small σ_α^2.

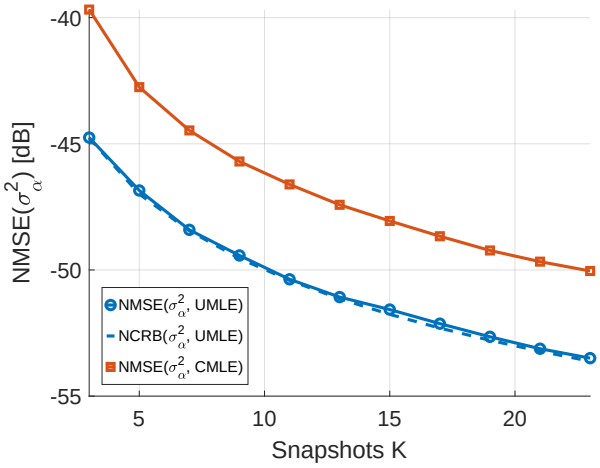

Figure 3: Comparison between CMLE and UMLE, with $\epsilon = 1$ ($\sigma_\alpha^2 = 0$) at $\text{SNR}_{\text{out}} = 20$ dB.

VI. Conclusions

In this study, an USM is proposed to collect more information from the complex amplitude in the context of DDM evaluations, along with time-delay estimation. For the proposed signal model, the corresponding ML estimators and closed-form expressions for the CRB were derived and validated through simulations. The main outcome is that the UMLE preserves the time-delay estimation performance of the CMLE, while also allowing access to more information. In fact, with that signal model, one can estimate σ_α^2 which is typically not observable in the CSM, and the phase and amplitude which are not observable in the standard zero mean USM. Notice that, for a given total power, the largest the ϵ, the smaller the error. This is due to the fact that the component σ_α^2, while possibly adding information of interest, also adds randomness to the signal. Overall, the CRB expressions give the ultimate achievable performance on the estimation of delay, and both mean and variance of a Gaussian source scattering, and the UMLEs are shown to be asymptotically efficient.

References

[1] V. U. Zavorotny, S. Gleason, E. Cardellach, and A. Camps, "Tutorial on remote sensing using GNSS bistatic radar of opportunity," *IEEE Geosci. Remote Sens. Mag.*, vol. 2, no. 4, pp. 8–45, Dec. 2014.

[2] S. G. Jin, E. Cardellach, and F. Xie, *GNSS Remote Sensing: Theory, Methods and Applications*. Dordrecht, Netherlands: Springer, 2014.

[3] P. J. G. Teunissen and O. Montenbruck, Eds., *Handbook of Global Navigation Satellite Systems*. Switzerland: Springer, 2017.

[4] S. Jin *et al.*, "Remote sensing and its applications using GNSS reflected signals: advances and prospects," *Satellite Navigation*, vol. 5, no. 1, Dec. 2024.

[5] C. Ruf and S. Gleason, "Spaceborne GNSS-R Bistatic Radar Remote Sensing, CYGNSS, and Future Missions," *Proceedings of the IEEE*, pp. 1–19, 2025.

[6] F. Martin *et al.*, "Mitigation of Direct Signal Cross-Talk and Study of the Coherent Component in GNSS-R," *IEEE Geoscience and Remote Sensing Letters*, vol. 12, no. 2, pp. 279–283, 2015.

[7] J. F. Munoz-Martin *et al.*, "Untangling the Incoherent and Coherent Scattering Components in GNSS-R and Novel Applications," *Remote Sensing*, vol. 12, no. 7, 2020.

[8] A. Camps, "Spatial Resolution in GNSS-R Under Coherent Scattering," *IEEE Geoscience and Remote Sensing Letters*, vol. 17, no. 1, pp. 32–36, 2020.

[9] M. M. Al-Khaldi *et al.*, "An Algorithm for Detecting Coherence in Cyclone Global Navigation Satellite System Mission Level-1 Delay-Doppler Maps," *IEEE Transactions on Geoscience and Remote Sensing*, vol. 59, no. 5, pp. 4454–4463, 2021.

[10] ——, "Inland Water Body Mapping Using CYGNSS Coherence Detection," *IEEE Transactions on Geoscience and Remote Sensing*, vol. 59, no. 9, pp. 7385–7394, 2021.

[11] I. M. Russo *et al.*, "Entropy-Based Coherence Metric for Land Applications of GNSS-R," *IEEE Transactions on Geoscience and Remote Sensing*, vol. 60, pp. 1–13, 2022.

[12] P. Zeiger *et al.*, "Analysis of CYGNSS coherent reflectivity over land for the characterization of pan-tropical inundation dynamics," *Remote Sensing of Environment*, vol. 282, 2022.

[13] J. Zhang *et al.*, "Mapping Surface Water Extents Using High-Rate Coherent Spaceborne GNSS-R Measurements," *IEEE Transactions on Geoscience and Remote Sensing*, vol. 60, pp. 1–15, 2022.

[14] E. Loria *et al.*, "Comparison of GNSS-R Coherent Reflection Detection Algorithms Using Simulated and Measured CYGNSS Data," *IEEE Transactions on Geoscience and Remote Sensing*, vol. 61, pp. 1–16, 2023.

[15] H. Carreno-Luengo *et al.*, "A New Multiresolution CYGNSS Data Product for Fully and Partially Coherent Scattering," *IEEE Transactions on Geoscience and Remote Sensing*, vol. 61, pp. 1–18, 2023.

[16] J. Peng *et al.*, "Signal Coherence and Water Detection Algorithms for the ESA HydroGNSS Mission," *IEEE Transactions on Geoscience and Remote Sensing*, vol. 62, pp. 1–18, 2024.

[17] O. Nogués i Cervelló *et al.*, "Improved GNSS-R altimetry methods: theory and experimental demonstration using airborne dual frequency data from the Microwave Interferometric Reflectometer (MIR)," *Remote Sensing*, vol. 13, no. 20, p. 4186, 2021.

[18] P. Stoica and A. Nehorai, "Performances study of conditional and unconditional direction of arrival estimation," *IEEE Trans. Acoust., Speech, Signal Process.*, vol. 38, no. 10, pp. 1783–1795, Oct. 1990.

[19] H. L. V. Trees, *Detection, estimation, and modulation theory: Part I*. New York, USA: Wiley, 1968.

[20] P. Das, J. Vilà-Valls, F. Vincent, L. Davain, and E. Chaumette, "A New Compact Delay, Doppler Stretch and Phase Estimation CRB with a Band-Limited Signal for Generic Remote Sensing Applications," *Remote Sensing*, vol. 12, no. 18, 2020.

[21] A. Renaux, P. Forster, E. Chaumette, and P. Larzabal, "On the high-SNR conditional maximum-likelihood estimator full statistical characterization," *IEEE Trans. Signal Process.*, vol. 54, no. 12, pp. 4840 – 4843, Dec. 2006.

[22] A. Renaux, P. Forster, E. Boyer, and P. Larzabal, "Unconditional Maximum Likelihood Performance at Finite Number of Samples and High Signal-to-Noise Ratio," *IEEE Trans. Signal Process.*, vol. 55, no. 5, pp. 2358–2364, 2007.

[23] M. I. Skolnik, *Radar Handbook*, 3rd ed. New York, USA: McGraw-Hill, 2008.

[24] F. Tupin, J. Inglada, and J. Nicolas, Eds., *Remote Sensing Imagery*. ISTE Ltd and John Wiley & Sons, 2014.

[25] L. Ortega, J. Vilà-Valls, and E. Chaumette, "Insights on the Estimation Performance of GNSS-R Coherent and Noncoherent Processing Schemes," *IEEE Geoscience and Remote Sensing Letters*, vol. 19, 2022.

[26] O. Besson, "Adaptive detection of rician targets," *IEEE Trans. Aerosp. Electron. Syst.*, vol. 59, no. 4, pp. 4700–4708, 2023.